RAPID COMMUNICATIONS

PHYSICAL REVIEW B VOLUME 45, NUMBER 21 1 JUNE 1992-I

Energetics of nanoscale graphitic tubules

D. H. Robertson, D. W. Brenner, and J. W. Mintmire
Naval Research Laboratory, Washington, D.C. 20375-5000
(Received 21 February 1992)

Using both empirical potentials and first-principles total-energy methods, we have examined the energetics and elastic properties of all possible graphitic tubules with radii less than 9 Å. We find that the strain energy per carbon atom relative to an unstrained graphite sheet varies as $1/R^2$ (where R is the tubule radius) and is insensitive to other aspects of the lattice structure, indicating that relationships derivable from continuum elastic theory persist well into the small-radius limit. We also predict that this strain energy is much smaller than that in highly symmetric fullerene clusters with similar radii, suggesting a possible thermodynamic preference for tubular structures rather than cage structures. The empirical potentials further predict that the elastic constants along the tubule axis generally soften with decreasing tubule radius, although with a distinct dependence on helical conformation.

The discovery by Krätschmer *et al.*[1] of a process for producing bulk quantities of fullerene clusters has opened up new opportunities for producing unique carbon-based materials. Among the possibilities are materials based on carbon fibers that have radii similar to that of C_{60}. For example, Iijima[2] has reported evidence of needlelike tubes consisting of concentric carbon fibers with radii as small as 22 Å forming at the negative end of an electrode in an apparatus typically used to produce fullerene clusters. If the synthesis and processing of these fibers can be precisely controlled, they may yield new materials with important structural and electronic properties.

Theoretical studies of these small-radii graphitic tubules have focused primarily on their electronic properties. Local-density functional[3] (LDF) and empirical tight-binding electronic structure calculations[4-6] predict that these materials will show conducting properties varying from metals to moderate band-gap semiconductors depending on their radii and helical arrangement of the carbon hexagons. In contrast to the electronic properties, relatively little has been reported regarding the lattice energetics and elastic properties of these structures. Such information may be helpful for optimizing the conditions necessary for producing subnanometer radii graphitic tubules with high strength-to-weight ratios.

We have examined the energetics of a set of tubules that can be constructed conceptually by rolling up a single sheet of graphite into a cylindrical tube with a constant radius. We report herein calculations for the energy and the force constant along the tubule axis for all such tubules with radii less than 9 Å using two related many-body empirical potentials. We find that the strain energy per carbon atom relative to an unstrained graphite sheet goes as $1/R^2$ (where R is the tubule radius) and is insensitive to other aspects of the lattice structure, indicating that relationships derivable from continuum elastic theory persist well into the small radius limit. These results are further supported by first-principles LDF calculations on a series of selected tubules. We also predict that the strain energy associated with infinitely extended tubules is much smaller than that for highly symmetric icosahedral fullerene clusters with similar average radii. We find that the force constants associated with stretching along the tubule axis decrease (i.e., the tubules become softer with decreasing radius). Unlike the strain energy, however, this force constant is sensitive to the helical structure of the tubule with the dependence increasing at smaller tubule radii.

We can visualize an infinite tubule as a conformal mapping of a two-dimensional honeycomb lattice (depicted in Fig. 1) to the surface of a cylinder that is subject to periodic boundaries both around the cylinder and along its axis. The proper boundary condition around the cylinder can only be satisfied if the circumference of the cylinder maps to one of the Bravais lattice vectors of the graphite sheet.[4] Thus each real lattice vector of the two-dimensional hexagonal lattice (the Bravais lattice for the honeycomb) defines a different way of rolling up the sheet into a tubule. Each such lattice vector, $\mathbf{R}$, can be defined in terms of the two primitive lattice vectors $\mathbf{R}_1$ and $\mathbf{R}_2$ and a pair of integer indices $[n_1,n_2]$, such that $\mathbf{R}=n_1\mathbf{R}_1+n_2\mathbf{R}_2$. The point-group symmetry of the honeycomb lattice will make many of these equivalent, however, so truly unique tubules are only generated using a one-twelfth irreducible wedge of the Bravais lattice. Within this wedge only a finite number of tubules can be constructed with a circumference below any given value such

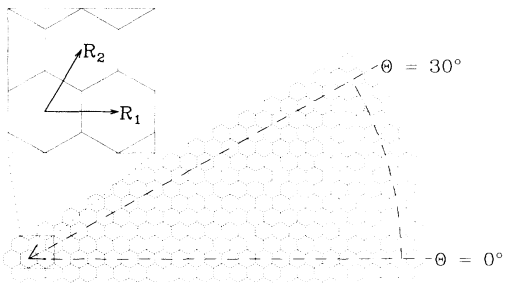


FIG. 1. Irreducible wedge of the graphite lattice. Primitive lattice vectors $\mathbf{R}_1$ and $\mathbf{R}_2$ are depicted in the inset. θ defines the angle that the circumference vector makes with the primitive lattice vector. The dashed lines depict the 9-Å cutoff for tubule structures.

 © 1992 The American Physical Society

as that shown by the dashed lines in Fig. 1.

The construction of the tubule from a conformal mapping of the graphite sheet allows us to make additional deductions about the tubule structure. Because the primitive reciprocal-lattice vectors of the hexagonal lattice (the Bravais lattice of the honeycomb lattice) are scalar multiples of real lattice vectors, the tubule can be shown to be translationally periodic down the tubule axis.[4] This feature allows us to use standard supercell techniques with periodic boundary conditions for our analysis of the lattice energetics. Each tubule can have up to three inequivalent helical operations derived from the primitive lattice vectors of the graphite sheet. Thus while *all* tubules will exhibit a helical structure, tubules constructed by mapping directions equivalent to $\theta=0°$ or 30° in Fig. 1 (which correspond to lattice translation indices of the form $[n,0]$ and $[n,n]$, respectively) to the circumference of the tubule will possess a reflection plane. These high-symmetry tubules will therefore be achiral. For convenience, we will denote these high-symmetry structures based on the shapes made by the most direct continuous path of bonds around the circumference of the tubule. We will denote the $[n,0]$-type structures as sawtooth, and the $[n,n]$-type structures as serpentine structures. For other values of θ, the tubules will be chiral and have three inequivalent primitive helical operations. By varying θ for tubules with similar radii, we can then ascertain which properties depend on the helical nature of the tubules.

We calculate the strain energy and stretching force constant of each tubule using two related many-body empirical potentials.[7,8] For both potentials the binding energy is given as

$$E_{\text{bind}}=\sum_i \sum_{j>i} [V_R(r_{ij})-B_{ij}V_A(r_{ij})] , \tag{1}$$

where r_{ij} is the scalar distance between atoms i and j, $V_R(r_{ij})$ and $V_A(r_{ij})$ represent a pair-additive core-core repulsion and an attraction due to valence electrons, respectively, and B_{ij} is a many-body empirical bond order that couples quantities such as bond angles and local coordination to the attractive potential. Tersoff[7] has shown that if Morse-like functions are used for the pair terms, a wide range of structural properties of solid-state carbon can be accurately modeled using this formalism. Furthermore, well-known trends relating bond length to total-energy and stretching force constants are reproduced, suggesting that this approach provides a reasonable starting point for predicting trends such as those studied here.

The two potentials used are both based on Eq. (1), but vary slightly in the form of B_{ij} and the parameters used in the pair terms. The first empirical potential (hereafter referred to as EP1) was introduced by Tersoff,[7] and was fit to the lattice constant and binding energy of a number of carbon lattices as well as the elastic constants and vacancy formation energies of graphite and diamond. This potential has recently been used by Hamada, Sawada, and Oshiyama[5] to generate tubule structures subsequently used in tight-binding electronic structure calculations. The second empirical potential (hereafter referred to as EP2) was developed in the context of a reactive hydrocarbon potential,[8] and has been fit to similar properties as EP1. Specific details of the two potential functions are given elsewhere.[7,8]

In addition to the empirical potential calculations, we have also calculated the electronic structure of a set of tubule structures using a first-principles, all-electron self-consistent LDF approach originally developed to treat chain polymers[9] and recently adapted for helical symmetry.[10] This method calculates the total energy and electronic structure using local Gaussian-type orbitals within a one-dimensional band-structure approach. The one-electron states are Bloch functions generated by repeated application of a screw operation, and belong to the irreducible representations of the screw symmetry group with a dimensionless analog of the wave vector k. Herein we used twenty-four evenly spaced points in the one-dimensional Brillouin zone ($-\pi<k\leq\pi$) and a carbon $7s3p$ Gaussian basis set.

We have examined all of the 169 tubules that can be constructed for radii less than 9 Å, assuming a carbon-carbon bond distance of 1.44 Å. We first generate an initial tubule structure with periodic boundary conditions matching the minimum translational periodicity along the tubule axis using the above-mentioned conformal mapping of the graphite sheet. Once these tubules are generated we relax the constraint of conformal mapping, and minimize the energy with respect to their configuration and periodic boundary along the tube axis for both these empirical potentials. Using this optimized structure we next calculate a numerical second derivative of the total energy with respect to strain along the tubule axis.

Figure 2 depicts the strain energy per atom (relative to that of the graphite sheet) for these tubules using optimized structures as a function of radius for both empirical potentials. As expected, for both potentials the strain energy decreases with larger radius, with the energy per atom approaching the limiting graphite value shown as the dashed line in Fig. 2. The results using EP1, however, show a larger dependence of the strain energy on tubule radii compared to the results using EP2. Although the results depicted in Fig. 2 are for tubules with θ values ranging from 0° to 30°, the strain energy appears to depend only on the radius and thus is independent of the chirality of the tubule.

We also calculated total energies for a series of high-symmetry tubules with $\theta=30°$ using first-principles LDF methods. These tubules all correspond to serpentine structures of the form $[n,n]$. The LDF electronic structure of the [5,5] structure has been presented elsewhere.[3] We have since found the minimum energy structure of this tubule by direct minimization of the total energy. The minimum energy structure is found to have a radius of 3.47 Å with both types of carbon-carbon bonds being essentially equal with lengths of 1.44 Å. Using unoptimized tubule structures generated from a conformal mapping of a graphite sheet with a 1.44-Å carbon-carbon bond distance, we have calculated the total energies of the [3,3], [4,4], [5,5], [6,6], [7,7], and [9,9] serpentine tubules. These values are plotted as open squares in Fig. 2. The strain energy is slightly larger than that predicted from either of the empirical potentials but shows a similar monotonically decreasing trend with increasing radius.

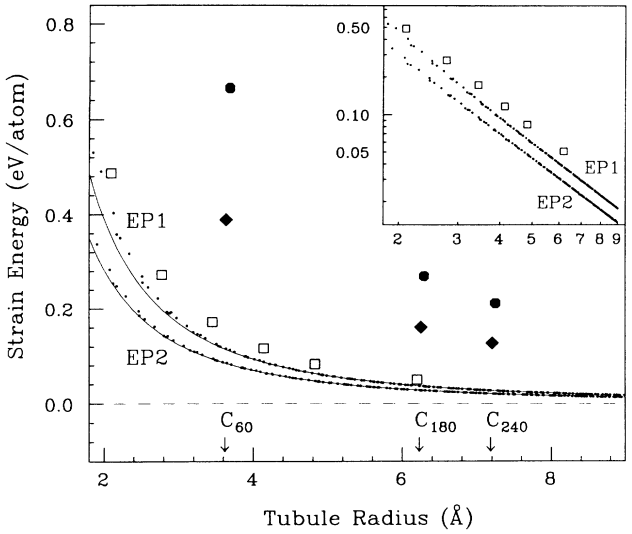


FIG. 2. Minimized strain energy relative to graphite (eV per carbon atom) as a function of tubule radius for potentials EP1 and EP2. Zero energy corresponds to the equilibrium graphite energies of -7.3995 and -7.3756 eV per atom for EP1 and EP2, respectively. The solid lines are the $1/R^2$ approximation resulting from the best linear fit to the log-log data given in the inset. The open squares give LDF strain energies for unoptimized serpentine structures relative to the extrapolated limit. The other symbols give corresponding strain energies per carbon atom using EP1 (circles) and EP2 (diamonds) for fullerene cage structures C_{60}, C_{180}, and C_{240} at the radii indicated.

This increased strain energy in the LDF results compared to the empirical potential results may arise from the explicit treatment of π-bonding energy in the LDF approach that is not incorporated in the empirical potentials.

Based on a continuum elastic model, Tibbetts[11] derived a strain energy for a thin graphitic tubule of the general form:

$$\sigma = \frac{\pi E L a^3}{12R}, \tag{2}$$

where E is the elastic modulus, R is the radius of curvature, L is the length of the cylinder, and a is a representative thickness of the order of the graphite interplanar spacing (3.35 Å). Assuming that the total number of carbon atoms is given by $N = 2\pi RL/\Omega$, where Ω is the area per carbon, we find that the strain energy per carbon is expected to be

$$\frac{\sigma}{N} = \frac{Ea^3}{24}\frac{\Omega}{R^2}. \tag{3}$$

The inset in Fig. 2 presents a log-log plot of the same tubule data presented in linear scale in the main portion of the figure. A linear regression using the natural logarithms of the data yields a slope of -2.0 ± 0.06 for both empirical potentials and the LDF results, with a high correlation coefficient. Using the results of this fit, we have drawn solid lines in the main portion of Fig. 2 showing how well the $1/R^2$ behavior fits the results for the empirical potentials. Thus we find that the $1/R^2$ dependence derived from continuum elastic theory[11,12] persists to very small radius tubules.

Also shown in Fig. 2 are the energies per atom with respect to graphite for the icosahedral fullerene clusters C_{60}, C_{180}, and C_{240} calculated using the respective empirical potentials. These clusters represent highly symmetric structures which have the strain energy well distributed around the cluster.[13] For both potentials the strain energy associated with these clusters is much larger than the infinite tubules with comparable radii, but should reduce to the graphite limit as the radius increases. This larger strain energy for the fullerenes reflects that while in tubules the curvature is restricted to one dimension perpendicular to the tubule axis, in fullerenes this curvature is present in two dimensions with respect to the flat graphite sheet. The formation of fullerene clusters rather than tubules during condensation may therefore be controlled by growth kinetics rather than energetics.

We have also examined the energetics of stretching and compressing a tubule. Figure 3 depicts total-energy results versus strain along the tubule axis for the [5,5] serpentine tubule, in which we compare results of fully optimized structures for a fixed repeat length along the tubule axis using both the empirical potentials and the LDF method. We see that both empirical methods are in good agreement both with each other and with the first-principles LDF results.

After this check on the reliability of the empirical potentials on calculating this effective elastic modulus of the tubule, we have extended our empirical potential calculations on the same set of 169 tubules used above for strain energies to the numerical second derivatives of the total energy with respect to strain along the tubule axis. These results (in terms of strain energy per carbon atom) are depicted in Fig. 4. Again, as the radii increase these values approach a limiting value. In the limit of infinite radius, we can correlate these results with elastic constants of graphite if we neglect interactions between layers. In this case our results for the second derivative of the total energy per carbon with respect to linear strain should just

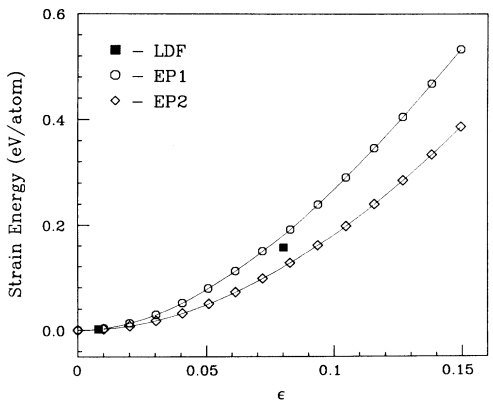


FIG. 3. Strain energy (eV per carbon atom) vs uniform tensile strain in the tubule axis direction for the [5,5] serpentine tubule using empirical potentials EP1 (open circles), EP2 (open diamonds), and the LDF method (solid squares). Solid lines for empirical potentials are used as guides to the eye.

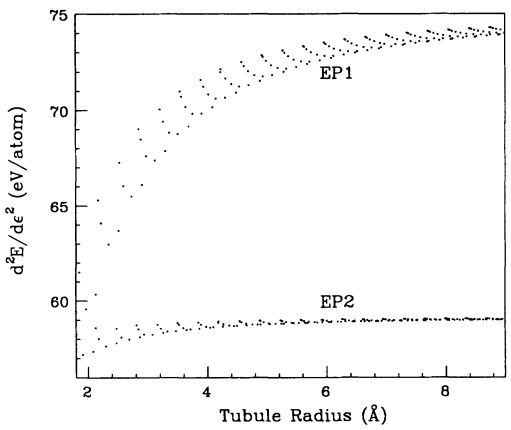


FIG. 4. Numerical second derivatives of energy per carbon with respect to uniform strain along the tubule axis direction for potentials EP1 and EP2.

equal the product of the graphite c_{11} elastic constant and the specific volume per carbon, V_0. Using experimentally determined lattice constants $a_0=2.462$ Å and $c_0=6.707$ Å, and the elastic constant $c_{11}=1.06$ TPa,[14,15] we find $V_0\approx 8.80$ Å^3 and $V_0c_{11}\approx 58.2$ eV/atom. This close agreement of EP2 with experiment and excess stiffness using the EP1 potential has been noted in other calculations on graphite systems.[7,16]

For both potentials, the tubules tend to get softer with smaller radii, with EP1 showing almost an order of magnitude greater dependence of the stiffness of the tubule as a function of radius than EP2. Unlike the energy, however, the stiffness of the tubules is dependent on θ as well as tubule radius and this dependence is maximized for the smaller, more strained tubules. We find that tubules with smaller θ are softer than those with a similar radius and larger value of θ. Thus the two achiral sawtooth ($\theta=0°$) and serpentine ($\theta=30°$) tubules yield the lower and upper limits of the stiffness along the tubular axis, respectively, for a given radius.

We have calculated the energies of optimized structures for all possible graphitic tubules with radii less than 9 Å using two different empirical potentials. We find a strain energy dependence on tubule radius of $1/R^2$ derived from continuum elastic theory even down to tubule radii of $\sim$3.5 Å, that typical of fullerene (C_{60}). LDF calculations for a series of serpentine tubules substantiate the former trend, but yield a somewhat larger strain energy. We also predict that this strain energy is much smaller than that in highly symmetric fullerene clusters with similar radii. The empirical potentials predict that as the radii of these tubules decrease the elastic constants along the tubule axis also decrease (i.e., the tubules become softer as their local curvature increases). Unlike the minimized energy, this elastic property shows a distinct dependence on θ with the largest variations with respect to θ occurring for small radii tubules. For similar radii, the lower and upper bounds of the stiffness are given by the achiral sawtooth and serpentine tubules, respectively.

This work was supported in part by the U.S. Office of Naval Research. Computational support for this project was provided in part by a grant of computer resources from the Naval Research Laboratory. D.H.R. acknowledges partial support from the NRC. We thank C. T. White and B. I. Dunlap for many helpful discussions.

[1] W. Krätschmer, L. D. Lamb, K. Fostiropoulos, and D. R. Huffman, Chem. Phys. Lett. **170**, 167 (1990); Nature (London) **347**, 354 (1990).

[2] S. Iijima, Nature (London) **354**, 56 (1991).

[3] J. W. Mintmire, B. I. Dunlap, and C. T. White, Phys. Rev. Lett. **68**, 631 (1992).

[4] J. W. Mintmire, D. H. Robertson, B. I. Dunlap, R. C. Mowrey, D. W. Brenner, and C. T. White, in *Electrical, Optical, and Magnetic Properties of Organic Solid State Materials,* edited by L. Y. Chiang, A. F. Garito, and D. J. Sandman, MRS Symposia Proceedings No. 247 (Materials Research Society, Pittsburgh, in press).

[5] N. Hamada, S. Sawada, and A. Oshiyama, Phys. Rev. Lett. **68**, 1579 (1992).

[6] R. Saito, M. Fujita, G. Dresselhaus, and M. S. Dresselhaus, Appl. Phys. Lett. (to be published).

[7] J. Tersoff, Phys. Rev. Lett. **61**, 2879 (1988); Phys. Rev. B **37**, 6991 (1988); Phys. Rev. Lett. **56**, 632 (1986).

[8] D. W. Brenner, Phys. Rev. B **42**, 9458 (1990).

[9] J. W. Mintmire and C. T. White, Phys. Rev. Lett. **50**, 101 (1983); Phys. Rev. B **28**, 3283 (1983).

[10] J. W. Mintmire, in *Density Functional Methods in Chemistry,* edited by J. Labanowski and J. Andzelm (Springer-Verlag, New York, 1991), pp. 125–138.

[11] G. G. Tibbetts, J. Cryst. Growth **66**, 632 (1983).

[12] J. S. Speck, M. Endo, and M. S. Dresselhaus, J. Cryst. Growth **94**, 834 (1989).

[13] B. I. Dunlap, D. W. Brenner, J. W. Mintmire, R. C. Mowrey, and C. T. White, J. Phys. Chem. **95**, 8737 (1991).

[14] B. T. Kelly, *Physics of Graphite* (Applied Science, London, 1981).

[15] M. S. Dresselhaus, G. Dresselhaus, K. Sugihara, I. L. Spain, and H. A. Goldberg, *Graphite Fibers and Filaments* (Springer-Verlag, Berlin, 1988).

[16] J. A. Harrison, R. J. Colton, C. T. White, and D. W. Brenner, in *Thin Films: Stresses and Mechanical Properties III,* edited by W. D. Nix, J. C. Bravman, E. Arzt, and L. B. Freund, MRS Symposia Proceedings No. 239 (Materials Research Society, Pittsburgh, in press); J. A. Harrison (private communication).